Supramolecular Photovoltaics

DOI: 10.1002/anie.201105133

Efficient Solution-Processed Bulk Heterojunction Solar Cells by Antiparallel Supramolecular Arrangement of Dipolar Donor–Acceptor Dyes**

Hannah Bürckstümmer, Elena V. Tulyakova, Manuela Deppisch, Martin R. Lenze, Nils M. Kronenberg, Marcel Gsänger, Matthias Stolte, Klaus Meerholz, and Frank Würthner**

Research on small-molecule-based organic semiconductors has undoubtedly been strongly influenced by xerographic photoconductors like triarylamines, the first important organic electronic materials in market products.[1] Their development was strongly influenced by the Bässler model, which provided a rationale for the design of amorphous organic photo- and semiconductors.[2] According to this model, only compounds that lack dipole moments are considered promising for charge-carrier transport because the increased energetic disorder associated with dipole moments is thought to impede charge hopping. Recently, we questioned this paradigm in the field of organic photovoltaics (OPV) and successfully implemented highly dipolar merocyanine dyes as active components for light harvesting as well as exciton and hole transport in solution-cast bulk heterojunction (BHJ) solar cells.[3] The rationale behind our concept[4] was that highly dipolar donor–acceptor (D–A) substituted π systems (also called push-pull dyes) self-assemble into centrosymmetric dimers,[5] thus effectively eliminating molecular dipole moments on the supramolecular and material levels.[6] Two drawbacks of our BHJ materials, however, limited the acceptance of our concept so far. Firstly, the best solar cells were obtained for merocyanine dyes whose molecular scaffolds were equipped with rather bulky substituents that interfere with close face-to-face antiparallel dimerization.[3] Secondly, the power-conversion efficiencies (η) under standard AM1.5, 100 mW cm^{-2} simulated solar illumination conditions for solution-cast BHJ cells with fullerenes—although significantly advanced by more sophisticated vacuum processing[7]—could not be improved beyond 2.6%, which is significantly lower than the best solution-processed small-molecule-based BHJ devices fabricated with A–D–A and D–A–D chromophores, for example, acceptor-substituted oligothiophenes (up to 3.7%)[8] and triarylamines (up to 4.3%),[9] diketopyrrolopyrroles (up to 4.4%),[10] and squaraines (up to 5.2%).[11] Herein, we introduce dipolar D–A dyes with flat structures that undoubtedly form centrosymmetric dimers[5] with perfectly cancelled dipole moments in the solid state. Solution-processed BHJ solar cells derived thereof exhibit power-conversion efficiencies up to 4.5–5.1% (dependent on light intensity), clearly placing D–A dyes now among the top-performing small molecules in the field of organic photovoltaics.

Scheme 1 outlines the synthetic route that follows our earlier work on merocyanine dyes for photorefractive materials[12] and the simple access to 5-dialkylamino-thiophene-2-carbaldehydes by Hartmann.[13] Detailed synthetic procedures and characterization data are described in the Supporting Information.

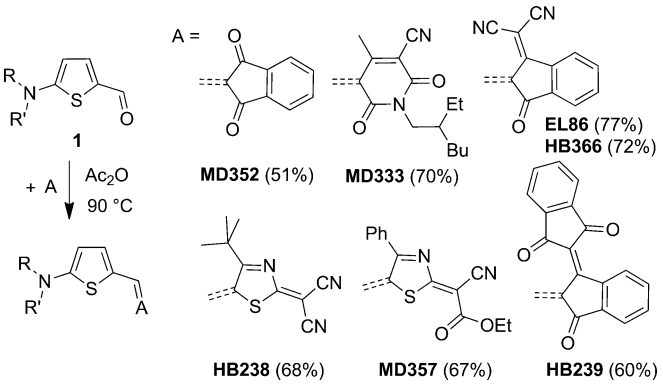

Scheme 1. Synthesis and molecular structures of the investigated D–A dyes (yields are given in parentheses). The substituents are R = *n*Bu and R′ = Et for **HB366** and R = R′ = *n*Bu for all other dyes.

The optical properties of the synthesized dyes were investigated by UV/Vis and electro-optical absorption spectroscopy.[14] Furthermore, cyclic voltammetry was performed for each dye to obtain information about their highest occupied molecular orbital (HOMO) and lowest unoccupied molecular orbital (LUMO) levels.[15] Figure 1a displays representative absorption spectra of the reported dye series in dichloromethane, and Figure 1b depicts the position of the frontier molecular orbital (FMO) energies of the chromophores with regard to the electron acceptor $PC_{61}BM$. The

[*] H. Bürckstümmer, Dr. E. V. Tulyakova, M. Deppisch, M. Gsänger, Dr. M. Stolte, Prof. Dr. F. Würthner
Universität Würzburg, Institut für Organische Chemie and Röntgen Research Center for Complex Material Systems
Am Hubland, 97074 Würzburg (Germany)
E-mail: wuerthner@chemie.uni-wuerzburg.de
M. R. Lenze, Dr. N. M. Kronenberg, Prof. Dr. K. Meerholz
Department of Chemistry, Universität zu Köln
Luxemburger Strasse 116, 50939 Köln (Germany)
E-mail: klaus.meerholz@uni-koeln.de

[**] We gratefully acknowledge funding of our project by the German Ministry of Science and Education (BMBF, OPEG project) and the German Science Foundation (DFG, priority programme SPP1355 "Elementary Processes of Organic Photovoltaics").

Supporting information for this article is available on the WWW under http://dx.doi.org/10.1002/anie.201105133.

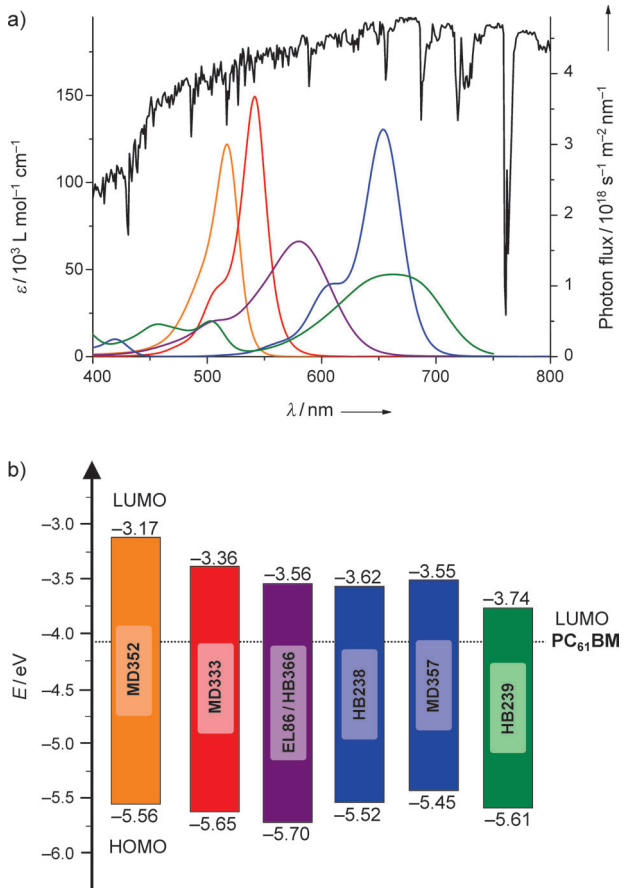

Figure 1. a) UV/Vis spectra of **MD352** (orange), **MD333** (red), **EL86** (violet), **MD357** (blue), and **HB239** (green) in CH_2Cl_2 ($c \approx 10^{-5}$ mol L^{-1}) at 298 K and solar photon flux at AM 1.5 conditions (black). The spectra of **HB366** and **HB238** are similar to those of **EL 86** and **MD357**, respectively; b) FMO levels and band gap (solid area) of dyes and their relative position to the LUMO of $PC_{61}BM$.

Table 1: Electro-optical and redox properties of investigated D–A dyes.

Dye	μ^2_{ag} [D^2][a]	$\mu^2_{ag} M^{-1}$ [D^2 mol g^{-1}]	μ_g [D][b]	$\Delta\mu$ [D][b]	E_{HOMO} [eV][c]	E_{LUMO} [eV][d]
MD352	82	0.22	5.7	4.2	−5.56*	−3.17
MD333	95	0.20	12.6	1.7	−5.65	−3.36
EL86	97	0.23	8.6	4.1	−5.70	−3.56
HB366	94	0.24	8.5	4.0	−5.69	−3.54
HB238	102	0.24	13.1	2.5	−5.52	−3.62
MD357	104	0.21	12.1	2.3	−5.45*	−3.55
HB239	74	0.15	6.1	4.6	−5.61*	−3.74

[a] UV/Vis measurements for dilute solution ($c \approx 10^{-5}$ M) in CH_2Cl_2 at 298 K. Absorption maxima (λ_{max}) and coefficients (ε) are given in the Supporting Information. [b] In 1,4-dioxane ($c \approx 10^{-6}$ M) at 298 K. [c] Calculated from CV measurements ($E_{1/2}{}^{ox}$/*E_p) in CH_2Cl_2 calibrated against the ferrocene/ferrocenium couple (Fc/Fc^+, −5.15 eV) as internal standard. [d] $E_{LUMO} = E_{HOMO} + (hc/\lambda_{max})$. * = Irreversible oxidation.

relevant electro-optical and electrochemical properties are summarized in Table 1.

Increasing the length of the polymethine chain and acceptor strength from indandione (**MD352**) to thiazole (**HB238**, **MD357**) and bis-indandione (**HB239**) based heterocycles entails a significant red-shift of the absorption maxima from 517 nm (**MD352**) to 654 nm (**MD357**) and 660 nm (**HB239**), respectively. Thus, by varying the acceptor unit, the absorption properties are tunable over the entire visible spectrum. The absorption coefficients at λ_{max} vary from approximately 5×10^4 L mol^{-1} cm^{-1} for **HB239** to approximately 1.5×10^5 L mol^{-1} cm^{-1} for **MD333** (Figure 1a). However, this result does not necessarily reflect the absorption strength of a chromophore since a dye with a sharp and intense absorption profile can absorb the same amount of photons as one with a broad, but less intense UV/Vis band. To evaluate the absorption strength, we define the figure-of-merit $\mu^2_{ag} M^{-1}$ (absorption density), which represents the transition dipole moment μ^2_{ag} divided by the molar mass M of the compound and is, therefore, directly related to the tinctorial strength of the respective dye. The absorption densities of the reported dyes all fall in the range of (0.22 ± 0.02) D^2 mol g^{-1}, except for **HB239**, which displays a significantly reduced tinctorial strength. If we apply the same procedure to determine the absorption density of P3HT (poly-3-hexylthiophene),[16] we obtain a distinctly lower value of only 0.14 D^2 mol g^{-1}. Regarding the electro-optical properties, we found that dyes **MD333**, **HB238**, and **MD357** show large ground-state dipole moments (μ_g) of 12–13 D and small changes of the dipole moment upon optical excitation ($\Delta\mu$), whereas **MD352**, **EL86**, **HB366**, and **HB239** exhibit distinctly lower μ_g and higher $\Delta\mu$ values. As expected,[12] the dyes close to the cyanine limit ($\Delta\mu = 0$ D)[17] show the largest transition dipole moments (Table 1).

Figure 1b illustrates one of the major benefits of D–A dyes with regard to organic solar cells: all dyes—even the low-bandgap ones—show favorable low-lying HOMO levels (−5.45 to −5.7 eV vs. vacuum). Low-lying HOMO levels enable high open-circuit voltages and are, therefore, desirable.[18] Within the presented dye series, the HOMO energies vary by only 0.25 eV. On the other hand, the respective acceptor unit has a significantly stronger influence on the LUMO level, which is shifted by 0.57 eV from **MD352** to **HB239**. Although the dyes with stronger acceptor units exhibit low-lying LUMO levels, the energy offsets from the dye LUMO levels to the LUMO of $PC_{61}BM$ are still close to the ideal value of 0.3–0.4 eV.[18b] Hence, the energetics of these dyes match ideally with $PC_{61}BM$ to minimize energy loss upon electron transfer from the donor dye to the fullerene acceptor. By modulating the acceptor unit, we are able to tune not only the absorption properties, but also the FMO levels of the respective chromophores.

For two characteristic dyes of our series, **EL86** and **HB239**, we have grown single crystals that could be resolved by single-crystal X-ray diffraction analysis.[19] As shown in Figure 2 and 3, the chromophores are located in planes parallel to each other arranged in discrete stacks. Each molecule features one close and one distant neighbor, hence forming close and distant centrosymmetric dimeric units. The C–C bond lengths of the methine bridges to the two heterocycles change only marginally, thus indicating fully conjugated π systems close to the cyanine limit.[12,17]

In the single-crystal structure of **EL86**, the molecule itself is only slightly distorted from planarity, with a torsion angle

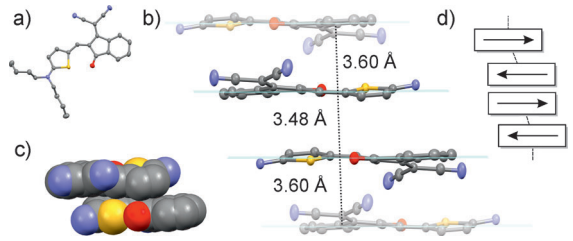

Figure 2. a) Molecular structure of **EL86** in the crystal. b) π stack of **EL86** with antiparallel packing motif. c) Space-filling view of the close dimer of **EL86** (alkyl chains and protons in (b) and (c) are omitted). d) Schematic representation of **EL86** stack showing the antiparallel orientation of the dipole moments (arrows).

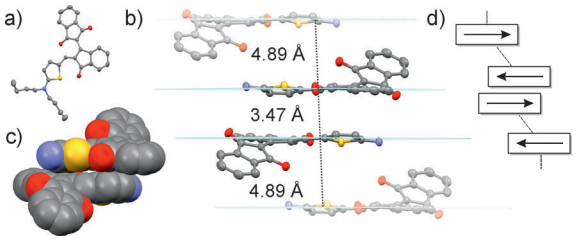

Figure 3. a) Molecular structure of **HB239** in the crystal. b) π stack of **HB239** with antiparallel packing motif. c) Space-filling view of the close dimer of **HB239** (alkyl chains and protons in (b) and (c) are omitted). d) Schematic representation of a **HB239** stack showing the antiparallel orientation of the dipole moments (arrows).

between the donor and acceptor unit of 13°. Within the stacks, almost equal distances of the close (3.48 Å) and the distant (3.60 Å) antiparallel neighbors result in a one-dimensional π stack of closely packed chromophores (Figure 2b). These show only small longitudinal displacements with respect to each other, thus leading to a pronounced contact area between the π surfaces of neighboring molecules. A tightly bound antiparallel dimer unit is also observed in the solid-state packing of **HB239** (3.47 Å distance); however, the distance to the other neighbor is significantly increased (4.89 Å) as shown in Figure 3b. Adjoining molecules in the close dimer also show a more pronounced longitudinal displacement with respect to each other, and transverse displacements are observed regarding the more distant neighbor, further reducing the π–π contact between adjacent molecules. Both effects are probably caused by the strongly distorted molecular structure of **HB239**, as the torsion angle between the two indandione units of the acceptor is 32°. Thus, the twisted acceptor moiety acts like a spacer between the centrosymmetric distant dimers and prevents the formation of a closely packed π stack as it is provided in the case of **EL86**.

The power conversion efficiency (η) of solar cells is defined as:

$$\eta = \frac{FF J_{SC} V_{OC}}{P_{in}} \quad (1)$$

where FF is the fill factor, J_{SC} the short-circuit current density, V_{OC} the open-circuit voltage, and P_{in} the power density of the incoming light. All described D–A dyes were evaluated in combination with the commonly used fullerene acceptor $PC_{61}BM$ in solution-processed BHJ solar cells using the simple device structure ITO/PEDOT:PSS (40 nm)/dye:$PC_{61}BM$/Al (120 nm) at an AM1.5 illumination intensity of 100 mW cm^{-2}. The dye:$PC_{61}BM$ layers were prepared by spin-coating and only optimized with respect to their layer thickness and the dye:$PC_{61}BM$ ratio. V_{OC} and FF were mostly unaffected by different dye:$PC_{61}BM$ ratios whilst J_{SC} and consequently η displayed maxima at a certain $PC_{61}BM$ content. Optimized film thicknesses were found to be 50–60 nm. A comparison of the solar cell characteristics is listed in Table 2, details on the device fabrication are given in the Supporting Information.

Table 2: Photovoltaic characteristics of chlorobenzene solution-cast dye:$PC_{61}BM$ BHJ solar cells for the optimized ratio.

Dye	λ_{max} [nm][b]	PCBM [wt%]	V_{OC} [V]	J_{SC} [mA cm^{-2}]	FF	η [%][c]
MD352	532	70	0.63	2.9	0.27	0.5
MD333	556	70	0.73	4.0	0.32	0.9
EL86	595	60	0.96	5.8	0.41	2.3
HB366[a]	595	55	0.94	8.3	0.38	3.0
HB238	682	75	0.72	4.5	0.35	1.1
MD357	689	70	0.47	4.0	0.27	0.5
HB239	700	75	0.68	4.0	0.36	1.0

[a] Cast from chloroform solution owing to solubility problems in chlorobenzene. [b] UV/Vis measurements of a thin film of the blend. [c] AM1.5 conditions, 100 mW cm^{-2}.

The open-circuit voltages determined for this series of dyes are centered at around 0.7 V. **MD357** shows the lowest V_{OC} of 0.47 V, which is consistent with this dye having the highest HOMO level within the series (Figure 1b). Likewise, the dyes with the lowest HOMO levels, **EL86** and **HB366**, give the highest V_{OC} of 0.94 and 0.96 V, respectively. The short-circuit current density is directly related to the light-harvesting efficiency as well as the charge-carrier properties of the active layer of a photovoltaic cell. Most devices investigated here have moderate J_{SC} values of approximately 4 mA cm^{-2}. Cells built with **MD352** exhibited a lower performance with a J_{SC} of 2.9 mA cm^{-2}, whereas significantly higher J_{SC} values of 5.8 and 8.3 mA cm^{-2} were determined for devices prepared with **EL86** and **HB366**, respectively. Notably, for these dyes, higher dye loadings resulted in the best solar cell performances. Fill factors of most devices were around 0.3, with the highest FF observed again for cells based on **EL86** and **HB366**. Accordingly, applying Equation (1), typical power-conversion efficiencies range between 0.5–1.1% with two clear outliers, the structurally very similar **EL86** and **HB366**, showing 2.3% and 3.0%, respectively.

Based on our initial results, several steps in the solar-cell fabrication were optimized with the best performing dye **HB366**. Whereas little effect was observed by post-treatments such as thermal annealing, clear improvements could be achieved by replacing $PC_{61}BM$ with $PC_{71}BM$ (enhanced absorption), replacement of the hole-collecting PEDOT:PSS layer by MoO_3, and applying a Ba/Ag metal electrode. The result of this optimization afforded a highly improved solar

cell with a power-conversion efficiency of 4.5% under standard AM1.5, 100 mW cm^{-2} conditions. Under reduced lighting conditions, an even higher efficiency of 5.1% was obtained (for details, see the Supporting Information). For a direct comparison, BHJ solar cells were also manufactured for Nguyen's diketopyrrolopyrrole (**DPP**, Figure 4), which is a

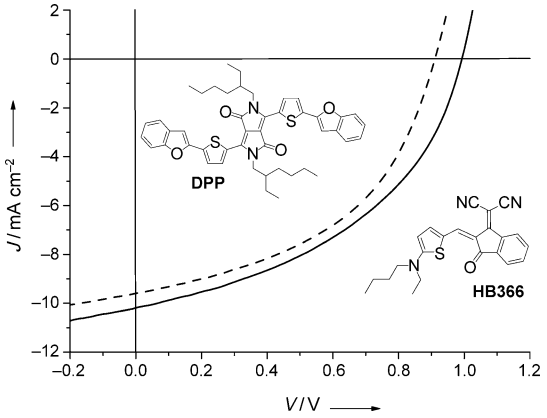

Figure 4. *J–V* response of the solar cells built with **HB366** (solid line, 55 wt% $PC_{71}BM$) and **DPP** (dashed line, 40 wt% $PC_{71}BM$) measured under simulated solar illumination (AM1.5, 100 mW cm^{-2}).

leading dye in the field of solution-processed small molecule BHJ solar cells.[10] Figure 4 compares the *J–V* curves of the optimized devices containing **HB366**/$PC_{71}BM$ and **DPP**/$PC_{71}BM$ as reference. Although we use significantly lower dye content (45 wt% compared to 60 wt%), a higher J_{SC} and V_{OC}, 10.2 mA cm^{-2} and 1.0 V, respectively, are observed for **HB366** compared to **DPP** (9.6 mA cm^{-2} and 0.91 V). The fill factors are quite similar (0.44 and 0.47, respectively), thus, the resulting power-conversion efficiency under standard conditions amounts to 4.5% for **HB366** and 4.1% for **DPP**.[20] Notably, devices that contain **DPP** need to be annealed at 110 °C for 10 min to reach this high performance, whereas cells built with **HB366** afford 4.5% without post treatment.

With this result, dipolar D–A dyes are now positioned among the most promising small molecules for organic photovoltaics despite the obvious contradiction with the Bässler model. To avoid large energetic disorder caused by their dipolarity, organization into favorable antiparallel aggregate structures is, however, crucial. This concept has been demonstrated in the solid state for dyes **EL86** and **HB239** that exhibit slightly different packing features, likely contributing to their varying performance in solar cells. While **EL86** assembles into π stacks with two close-by antiparallel neighbor molecules, such favorable packing is impeded for **HB239** because of steric hindrance. Attempts to measure the hole mobility of **HB239** in organic field-effect transistors (OFETs) failed for both, pristine films and blends with $PC_{61}BM$. In contrast, for **EL86**, hole mobilities of 1×10^{-5} cm^2 V^{-1} s^{-1} and 1×10^{-6} cm^2 V^{-1} s^{-1} were measured for pure films and blends with $PC_{61}BM$, respectively. Slightly reduced values were obtained for the structurally related **HB366** (0.7×10^{-5} cm^2 V^{-1} s^{-1} and 0.9×10^{-6} cm^2 V^{-1} s^{-1}). Even higher hole mobilities were measured for spin-coated films of the dye **HB238** (4×10^{-4} cm^2 V^{-1} s^{-1}), which exhibits the largest dipole moment within our series (Table 1). Interestingly, these values are not much smaller than those of amorphous nondipolar triarylamine-based photoconductors.[1,2] As our results indicate, charge-transport properties are not necessarily impaired by large ground-state dipole moments of monomeric molecules, if the molecules are assembled in a suitable fashion in the bulk material.

In conclusion, this study provides a strong impetus to reconsider established design concepts in organic semiconductor research, particularly in the area of small-molecule-based OPV, but also beyond (i.e. in other areas of organic electronics or polymeric OPV as well). Our studies show that highly dipolar D–A dyes are applicable as p-type hole-conducting components in BHJ solar cells. These cells have been optimized in a rather short time to reach power-conversion efficiencies similar to those obtained with established nonpolar small-molecule materials. Thus, a serious restriction in the design of small molecules for OPV has been overcome, opening investigation up to a much larger variety of chemical structures. For us and other researchers working on optoelectronic applications of push-pull chromophores, it may appear as an odd anecdote that these dyes widely failed in nonlinear optical applications despite their outstanding suitability on the molecular level owing to dipolar aggregation in the bulk, which has now shown to be the pathway to success in OPV.

Received: July 21, 2011
Revised: September 9, 2011
Published online: October 14, 2011

Keywords: aggregation · centrosymmetric dimers · dyes/pigments · merocyanines · organic solar cells

[1] D. S. Weiss, M. Abkowitz, *Chem. Rev.* **2010**, *110*, 479–526.
[2] a) A. Dieckmann, H. Bässler, P. M. Borsenberger, *J. Chem. Phys.* **1993**, *99*, 8136–8141; b) D. Hertel, H. Bässler, *ChemPhysChem* **2008**, *9*, 666–688.
[3] a) N. M. Kronenberg, M. Deppisch, F. Würthner, H. W. A. Lademann, K. Deing, K. Meerholz, *Chem. Commun.* **2008**, 6489–6491; b) H. Bürckstümmer, N. M. Kronenberg, M. Gsänger, M. Stolte, K. Meerholz, F. Würthner, *J. Mater. Chem.* **2010**, *20*, 240–243; c) H. Bürckstümmer, N. M. Kronenberg, K. Meerholz, F. Würthner, *Org. Lett.* **2010**, *12*, 3666–3669.
[4] F. Würthner, K. Meerholz, *Chem. Eur. J.* **2010**, *16*, 9366–9373.
[5] a) F. Würthner, S. Yao, *Angew. Chem.* **2000**, *112*, 2054–2057; *Angew. Chem. Int. Ed.* **2000**, *39*, 1978–1981; b) F. Würthner, S. Yao, T. Debardemaeker, R. Wortmann, *J. Am. Chem. Soc.* **2002**, *124*, 9431–9447.
[6] For feature articles on other supramolecular concepts in organic photovoltaics, see: a) D. M. Bassani, L. Jonusauskaite, A. Lavie-Cambot, N. D. McClenaghan, J. L. Pozzo, D. Ray, G. Vives, *Coord. Chem. Rev.* **2010**, *254*, 2429–2445; b) R. Bhosale, J. Misek, N. Sakai, S. Matile, *Chem. Soc. Rev.* **2010**, *39*, 138–149; c) J. L. Delgado, P.-A. Bouit, S. Filippone, M. A. Herranz, N. Martín, *Chem. Commun.* **2010**, *46*, 4853–4865; d) M. V. Martínez-Díaz, G. de La Torrea, T. Torres, *Chem. Commun.* **2010**, *46*, 7090–7108.
[7] N. M. Kronenberg, V. Steinmann, H. Bürckstümmer, J. Hwang, D. Hertel, F. Würthner, K. Meerholz, *Adv. Mater.* **2010**, *22*, 4193–4197.

[8] B. Yin, L. Yang, Y. Liu, Y. Chen, Q. Qi, F. Zhang, S. Yin, *Appl. Phys. Lett.* **2010**, *97*, 023303. For more sophisticated vacuum-processed BHJ solar cells with better performance, see: R. Fitzner, E. Reinold, A. Mishra, E. Mena-Osteritz, H. Ziehlke, C. Körner, K. Leo, M. Riede, M. Weil, O. Tsaryova, A. Weiß, C. Uhrich, M. Pfeiffer, P. Bäuerle, *Adv. Funct. Mater.* **2011**, *21*, 897 – 910.

[9] H. Shang, H. Fan, Y. Liu, W. Hu, Y. Li, X. Zhan, *Adv. Mater.* **2011**, *23*, 1554 – 1557.

[10] B. Walker, A. B. Tamayo, X.-D. Dang, P. Zalar, J. H. Seo, A. Garcia, M. Tantiwiwat, T.-Q. Nguyen, *Adv. Funct. Mater.* **2009**, *19*, 3063 – 3069.

[11] G. Wei, S. Wang, K. Sun, M. E. Thompson, S. R. Forrest, *Adv. Eng. Mater.* **2011**, *2*, 184 – 187.

[12] a) F. Würthner, R. Wortmann, K. Meerholz, *ChemPhysChem* **2002**, *3*, 17 – 31; b) S. R. Marder, B. Kippelen, A. K. Y. Jen, N. Peyghambarian, *Nature* **1997**, *388*, 845 – 851; c) M. Blanchard-Desce, R. Wortmann, S. Lebus, J.-M. Lehn, P. Krämer, *Chem. Phys. Lett.* **1995**, *243*, 526 – 532.

[13] H. Hartmann, S. Scheithauer, *J. Prakt. Chem.* **1969**, *311*, 827 – 843.

[14] W. Liptay, *Excited States*, *Vol. 1* (Ed.: E. C. Lim), Academic Press, New York, **1974**, p. 129.

[15] N. G. Connelly, W. E. Geiger, *Chem. Rev.* **1996**, *96*, 877 – 910.

[16] For polymers, the absorption coefficient ε is calculated per monomer unit, that is, $M = 166.3\ \mathrm{g\,mol^{-1}}$ for P3HT. For details, see the Supporting Information.

[17] The cyanine limit is the point where a π-conjugated push-pull dye exhibits equal ground- and excited-state dipole moments and concomitantly the smallest reorganization upon optical excitation. For details, see Ref. [12a].

[18] a) A. Cravino, *Appl. Phys. Lett.* **2007**, *91*, 243502; b) G. Dennler, M. C. Scharber, C. J. Brabec, *Adv. Mater.* **2009**, *21*, 1323 – 1338.

[19] For details of the crystal structures, see the Supporting Information; CCDC 835848 (**EL86**) and 835849 (**HB239**) contain the supplementary crystallographic data for this paper. These data can be obtained free of charge from The Cambridge Crystallographic Data Centre via www.ccdc.cam.ac.uk/data_request/cif.

[20] In Ref. [10], slightly higher values have been achieved for this DPP derivative, that is, $V_{OC} = 0.92$ V, $J_{SC} = 9.6\ \mathrm{mA\,cm^{-2}}$, and $\eta = 4.4\,\%$.

